Scaling, phase transitions, and nonuniversality in a self-organized critical cellular-automaton model

Kim Christensen* and Zeev Olami
Department of Physics, Brookhaven National Laboratory, Upton, New York 11973
(Received 20 December 1991)

We present a two-dimensional continuous cellular automaton that is equivalent to a driven spring-block model. Both the conservation and the anisotropy in the model are controllable quantities. Above a critical level of conservation, the model exhibits self-organized criticality. The self-organization of this system and hence the critical exponents depend on the conservation and the boundary conditions. In the critical isotropic nonconservative phase, the exponents change continuously as a function of conservation. Furthermore, the exponents vary continuously when changing the boundary conditions smoothly. Consequently, there is no universality of the critical exponents. We discuss the relevance of this for earthquakes. Introducing anisotropy changes the scaling of the distribution function, but not the power-law exponent. We explore the phase diagram of this model. We find that at low conservation levels a localization transition occurs. We see two additional phase transitions. The first is seen when moving from the conservative into the nonconservative model. The second appears when passing from the anisotropic two-dimensional system to the purely one-dimensional system.

PACS number(s): 05.40.+j, 05.45.+b

I. INTRODUCTION

The common appearance of fractal structures in nature is a long-standing puzzle. How can systems that interact only locally create correlated structures with a great variety of length scales and scale invariance? We encounter this phenomenon in statistical physics when a phase transition takes place in an equilibrium system. The system exhibits fluctuations in all possible length scales, but the phase transition occurs only at a critical point, to which one has to fine-tune some external parameters of the system. Obviously, there is no reason to assume that natural systems are fine-tuned to a thermodynamic phase-transition point.

Recently, Bak, Tang, and Wiesenfeld (BTW) suggested that natural systems might organize themselves, without any fine-tuning, to a critical state through their local dynamics [1]. They named this kind of organization to criticality "self-organized criticality" (SOC). This behavior is usually characterized by a power-law distribution function of the activity (avalanches) in the critical dynamical system and by existence of scale invariance of the distribution function.

The idea of SOC went hand in hand with a definite cellular-automaton algorithm, suggested by BTW, initiating enormous scientific activity. Various different cellular automata were studied and a great effort was spent on deriving some theoretical understanding of the new models.

A common feature to most of the models was that the local dynamical rules obeyed a conservation law. There has been some question as to whether or not the conservation is a necessary requirement for SOC [2,3]. With regard to the generality of the concept of SOC, this is a critical aspect, since many natural phenomena have inherent nonconservative properties.

Simulation of a system, with local perturbations and nonconservation in the dynamical rules of the original BTW model, shows that a length scale is indeed introduced into the problem [4]. At the same time different models with some degree of local nonconservation, like the "game of life" and "forest fire model," seem to be critical. However, it is very hard to follow the dynamics in detail in those models. In fact, the local dynamics can be "more than conservative," so the average nonconservation in the latter models is not well defined; thus it is not clear to what extent the SOC is associated with the requirement of conservation.

Recently, Feder and Feder introduced a two-dimensional model (hereafter called the Feder model) with low level of nonconservation that seems to display criticality [5]. While this result is indeed very intriguing, the model suffers from several deficiencies. One is that without dynamical noise the model behaves periodically, showing no criticality. Even with noise, where the model exhibits criticality, the model behaves almost periodically. Also, the amount of nonconservation is not a fully controllable quantity, and it is somewhat unclear what the role of the nonconservation is.

Another general question concerns the universality of the models. An attempt to connect the problem of SOC to randomly driven Langevin equations was made by several authors [2,3]. The basic equations were directed nonlinear diffusion equations driven by random noise. The primary predictions of those models are that any kind of nonconservation will immediately destroy criticality and that a limited set of universal exponents will characterize the systems. It is doubtful whether the models based on differential equations have any connection to SOC due to the different nature of the dynamical rules. Moreover, the result of Feder and Feder [5] question the application of differential equations to this kind of prob-

lem. Still, it is quite interesting to see if the predictions based on nonlinear differential equations have any relevance to critical cellular-automata models.

We must notice that fractal behavior in nature usually does not display universality and in most relevant phenomena a great variety of exponents are seen. Two simple examples are the power-law distributions of energy released during an earthquake, which will be discussed later (Sec. IV), and the power-law distributions of "$1/f$ noise." No universal power-law exponent characterize either case.

If there exist any universality classes in the cellular-automata models, there are obviously a large number of them. It seems that almost any modification of the algorithms introduces different exponents [6,7]. Even small modifications of the original BTW model that leave all the symmetries the same, for example, can change the scaling and the exponents [8]. This might be related to the observed variance in the critical exponents.

In this paper we introduce a generalized continuous cellular-automaton model where the nonconservation is a controlled quantity [9,10]. This model has several fascinating aspects.

First, it can be directly mapped into the Burridge-Knopoff spring-block model of earthquakes [11]. Hence the relevant variables can be interpreted as the forces in a spring-block system and the nonconservation is simply defined by a ratio between the elastic constants. Though the motivation for the model is derived from the Burridge-Knopoff spring-block model, it can be regarded as a generic representation of a nonconservative system.

Second, this model displays SOC over a very wide range of conservation levels. That is, we observe power-law distributions for the relevant physical quantities, where the cutoff scales with the size of the system. Furthermore, we find that the level of conservation has an impact on the power laws and the scaling exponents of this system. In particular, this has implications for the power-law distributions of earthquakes.

Third, two phase transitions are observed for this model. The first transition, where the scaling of the avalanches changes discontinuously, occurs when going from the conservative into the nonconservative case. A second phase transition takes place in low conservation levels, where we observe a localization of the avalanches. Between the two phase transitions the exponents change continuously.

Fourth, we find that the isotropic version of our model displays a continuous transition from two-dimensional to one-dimensional scaling. But the impact on the power law is negligible.

Finally, we find that a change of boundary conditions has an effect on the criticality and the exponents. For two natural choices of boundary conditions of the Burridge-Knopoff model we find large differences between the exponents. The boundary of the system has a strong influence on the self-organization process; consequently it affects the critical exponents.

In Sec. II we describe how the model is derived from the Burridge-Knopoff spring-block model and discuss the difference between our model and related models. We define the critical power-law exponent, and the critical scaling indices are introduced in the concept of finite-size-scaling analysis. In Sec. III we present a detailed study of the exponents and the finite-size scaling of the isotropic model in two dimensions. We observe several phase transitions and a variability of the scaling exponents inside the critical phases. We present results for the free boundary conditions of the spring-block model, and some observations on the variability of the laws as a function of the boundary conditions. In Sec. IV we consider the relationship of our results to earthquakes. Finally, we discuss the anisotropic model and the complete phase diagram of this model in Sec. V. In conclusion, we interpret our results in a wider context.

II. THE CELLULAR-AUTOMATON MODEL, EXPONENTS, AND FINITE-SIZE SCALING

A. Derivation of the model

Our model can be considered as a general nonconservative cellular automaton; hence our results have general implications. However, it is important to notice that it can be related directly to a driven model of earthquakes. Therefore, we begin by deriving this model from the simplified model suggested by Burridge and Knopoff for the internal dynamics of one single fault.

We consider a two-dimensional version of their model where the fault is represented by a two-dimensional network of blocks interconnected by springs. Each block is connected to the four nearest neighbors. Additionally, each block is connected to a single rigid driving plate by another set of springs, as well as connected frictionally to a fixed rigid plate [see Fig. 1(a)]. The blocks are driven by the relative movement of the two rigid plates. When the force on one of the blocks is larger than some threshold value $F_{\rm th}$ (the maximal static friction), the block slips. We assume that the moving block will slip to the zero-force position. The slip of one block will redefine the forces on its nearest neighbors. This can result in further slips and a chain reaction (an avalanche) can evolve.

We define an $L \times L$ array of blocks by (i,j) where i,j are integers $1 \le i,j \le L$. The displacement of each block from its relaxed position on the lattice is defined as $x_{i,j}$. The total force exerted by the springs on a given block (i,j) is expressed by

$$F_{i,j} = K_1[2x_{i,j} - x_{i-1,j} - x_{i+1,j}] + K_2[2x_{i,j} - x_{i,j-1} - x_{i,j+1}] + K_L x_{i,j} , \quad (1)$$

where K_1, K_2, and K_L denote the elastic constants [see Fig. 1(b)]. When the two rigid plates move relative to each other, the total force on each block increases uniformly (with a rate proportional to $K_L V$, where V is the relative velocity between the two rigid plates) until one site reaches the threshold value and the process of relaxation begins (an earthquake is triggered). It can easily be shown (see Appendix A) that the redistribution of forces after a local slip at the position (i,j) is given by the relation

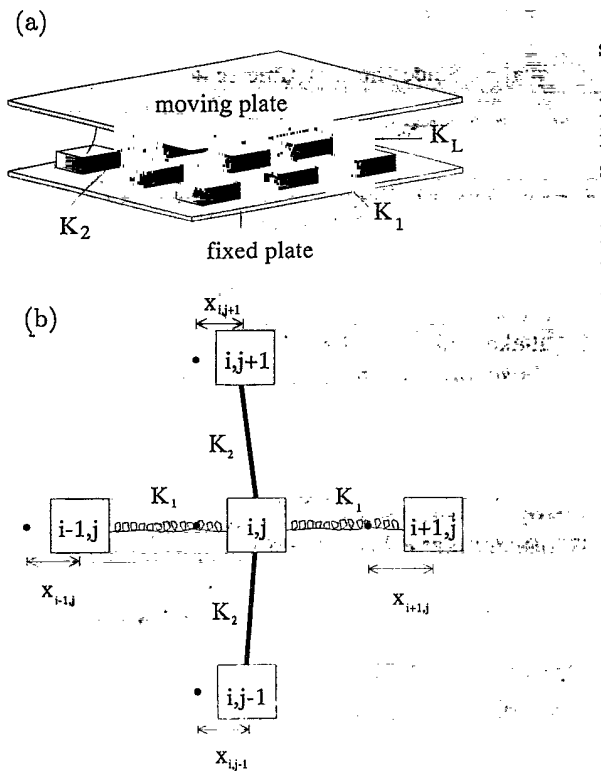

FIG. 1. The geometry of the Burridge-Knopoff spring-block model: (a) The two-dimensional system of blocks connected by springs. The force on the blocks increases uniformly as a response to the relative movement of the rigid plates. (b) A detailed picture of a given block (i,j) and its surroundings.

$$F_{i\pm1,j}\rightarrow F_{i\pm1,j}+\delta F_{i\pm1,j}\ ,$$
$$F_{i,j\pm1}\rightarrow F_{i,j\pm1}+\delta F_{i,j\pm1}\ , \tag{2}$$
$$F_{i,j}\rightarrow 0\ ,$$

where the increase in the force on nearest-neighbor blocks is

$$\delta F_{i\pm1,j}=\frac{K_1}{2K_1+2K_2+K_L}F_{i,j}=\alpha_1 F_{i,j}\ ,$$
$$\delta F_{i,j\pm1}=\frac{K_2}{2K_1+2K_2+K_L}F_{i,j}=\alpha_2 F_{i,j}\ . \tag{3}$$

For simplicity we denote the elastic ratios by α_1 and α_2, respectively. Notice that this relaxation rule is very similar to the BTW model [1]. However, when $K_L>0$, the redistribution of the force is nonconservative. In the context of the BK model, $K_L>0$; otherwise, no driving force is possible. In the context of continuous cellular automata, it is obviously of interest to check the full possible range of parameters. Since the amount of nonconserved force is $(1-2\alpha_1-2\alpha_2)F_{i,j}$, we define the level of conservation as $2\alpha_1+2\alpha_2$. However, with respect to the energy the model is nonconservative even if the redistribution of force is conservative. We emphasize that the terminology "conservative" and "nonconservative" refers to the redistribution of forces.

Some differences between our model and other models should be noticed.

(1) The force on the critical site is set to zero when relaxed. The same rule is used by Feder and Feder, while in the BTW model, a constant amount (usually $F_{\rm th}$) is subtracted.

(2) The redistribution of force to the neighbors is proportional to the force in the relaxing site. In the Feder and the BTW models this is not the case: A constant amount (usually 1) is transferred to the nearby sites.

(3) The BTW model is conservative, unlike the Feder model, where the amount of nonconservation is $F_{i,j}-F_{\rm th}$, where $F_{i,j}$ is the relaxing site. The nonconservation in our model is proportional to $F_{i,j}$.

(4) This model, as well as the Feder model and the model suggested by Bak and Tang [12] and Bak and Chen [13] for description of earthquakes, is globally driven, i.e., the full bulk is raised simultaneously. This driving is a natural choice for models representing earthquakes or other globally driven systems. This is a very important point since random local driving can destroy the correlations and the self-organization of the system. Furthermore, we must note that we see no direct relationship between the latter three models and the two-dimensional Burridge-Knopoff spring-block model.

(5) If $K_1\neq K_2$ ($\alpha_1\neq\alpha_2$), this model is also anisotropic. We can control the amount of anisotropy by changing the ratio between α_1 and α_2. In the extreme case the system will be one dimensional.

B. Scaling and SOC

It is very important to investigate how the finite size of the system affects the properties we measure. The trademark of SOC is the existence of a power-law distribution function of the avalanche sizes that scale with the system size. We concentrate our effort on the avalanche-size distribution, where the size is defined by the total number of relaxations in a single avalanche. It was found that this number is also proportional to the released strain (energy) in the system. Let $P(E,L)$ be the probability density of having an avalanche of size E in a system of linear size L. If the distribution function (note that we use the concept "distribution function" as equivalent to "probability density" although the two terms are not mathematically equivalent) is a power law, we define the power-law exponent B:

$$P(E,L)\sim E^{-(1+B)}\ . \tag{4}$$

The scaling properties of the system are investigated by *finite-size-scaling* analysis—that is, we make the ansatz that the probability density scales with system size as

$$P(E,L)=L^{-\beta}g(E/L^{\nu})\ , \tag{5}$$

where g is a so-called universal *scaling function* and β and ν are critical indices describing the scaling of the distribution function. The critical index ν expresses how the finite-size cutoff scales with system size, while the critical index β is related to the normalization (or rather renormalization) of the distribution function.

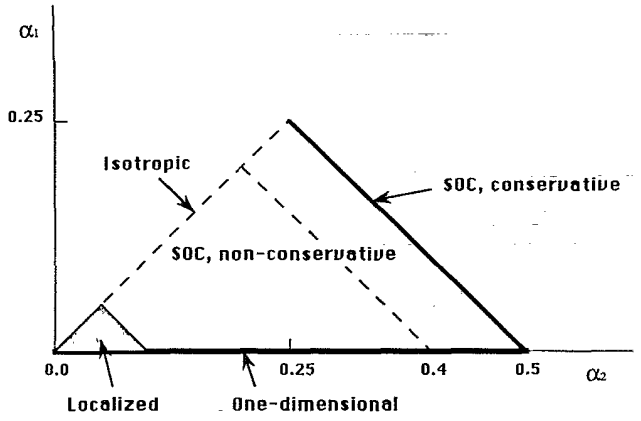

FIG. 2. The phase diagram for the model. When the level of conservation $2\alpha_1+2\alpha_2<1$, the system is nonconservative. If $\alpha_1=\alpha_2=\alpha$, the model is isotropic. Finally, when $\alpha_1=0$, $\alpha_2\neq 0$, the system is purely one dimensional.

If the distribution function is a power law, it is easy to show the following relation between the exponents (see, for example, Ref. [6]):

$$1+B=\beta/\nu\ . \tag{6}$$

We will measure the three exponents B, ν, and β systematically in different points (α_1,α_2) of the phase diagram of the model (see Fig. 2).

C. Definition of boundary conditions

The boundary is an integrated part of any finite system. The model would not be well defined without a specification of the boundary conditions. There is a very large range of possible boundary conditions. We can control the properties of the boundary by changing the α at the boundary, henceforth called $\alpha_{\rm BC}$. As we will show later, the system is sensitive to the nature of the boundary.

For the spring-block problem there are two extreme possibilities: (a) The blocks in the boundary layer are connected only to blocks within the faults, implying $\alpha_{\rm BC}=\alpha/(1-\alpha)$; the boundary is *free*. (b) The blocks in the boundary layer are coupled to an imaginary boundary block by springs, $\alpha_{\rm BC}=\alpha$; the boundary is *open*. We refer to Appendix B for a detailed discussion of those boundary conditions. Notice that the free boundary conditions are more conservative than the open boundary conditions. Neither the free nor the open boundary conditions are probably physically realistic, but the actual boundary conditions must be in between the two extreme limits. In the context of continuous cellular-automata models, one can even introduce a totally conservative boundary condition, $\alpha_{BC}=\frac{1}{3}$, which we will denote as a *reflecting* boundary.

III. SIMULATION OF THE MODEL

The rules for the driving of our model are motivated by the dynamics of earthquakes. There are two time scales involved. One is defined by the motion of the tectonic plates, and the other is the actual duration of an earthquake. Since the first time scale is much larger than the second, we can separate the time scales. We consider the earthquake as instantaneous and do not drive the system during an avalanche. Thus the algorithm for simulating the system is the following: Define random initial forces in the system. Strain is accumulated uniformly across the system as the rigid plates move. When the force on a certain site is above the threshold value $F_{\rm th}$, this site will relax according to Eqs. (2) and (3). The triggered earthquake will stop when there are no sites left with a force above the threshold. Strain starts to accumulate once again. The system organizes into the critical state after a transient time which is proportional to the system volume but dependent on the level of conservation. We collect the statistics only after the system is organized. We continue this process to get proper statistics of the distribution function of the energy released (which is proportional to the total number of relaxations) during the earthquakes. The results that are presented in this

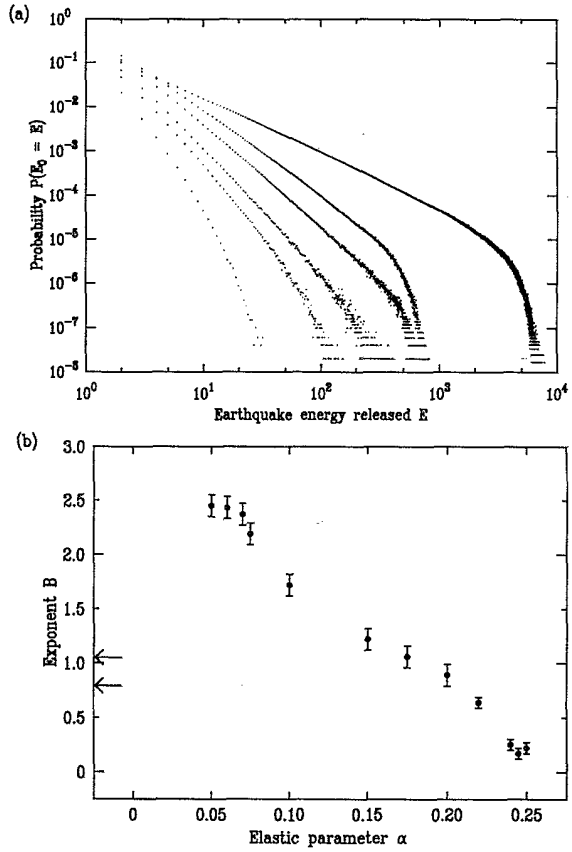

FIG. 3. (a) Simulation results for a 35×35 system with open boundary conditions. Different curves refer to different levels of conservation. The slopes of the curves become steeper as the α values are decreased. The graphs correspond to $\alpha=0.25$, 0.20, 0.15, 0.10, 0.075, and 0.025, respectively. Notice that the last point is not critical. (b) The power-law exponent B as a function of the elastic parameter α defined in Eq. (3). Below $\alpha=0.05$, there is a transition to exponential decay. The arrows indicate the actual measured B values for earthquakes [15].

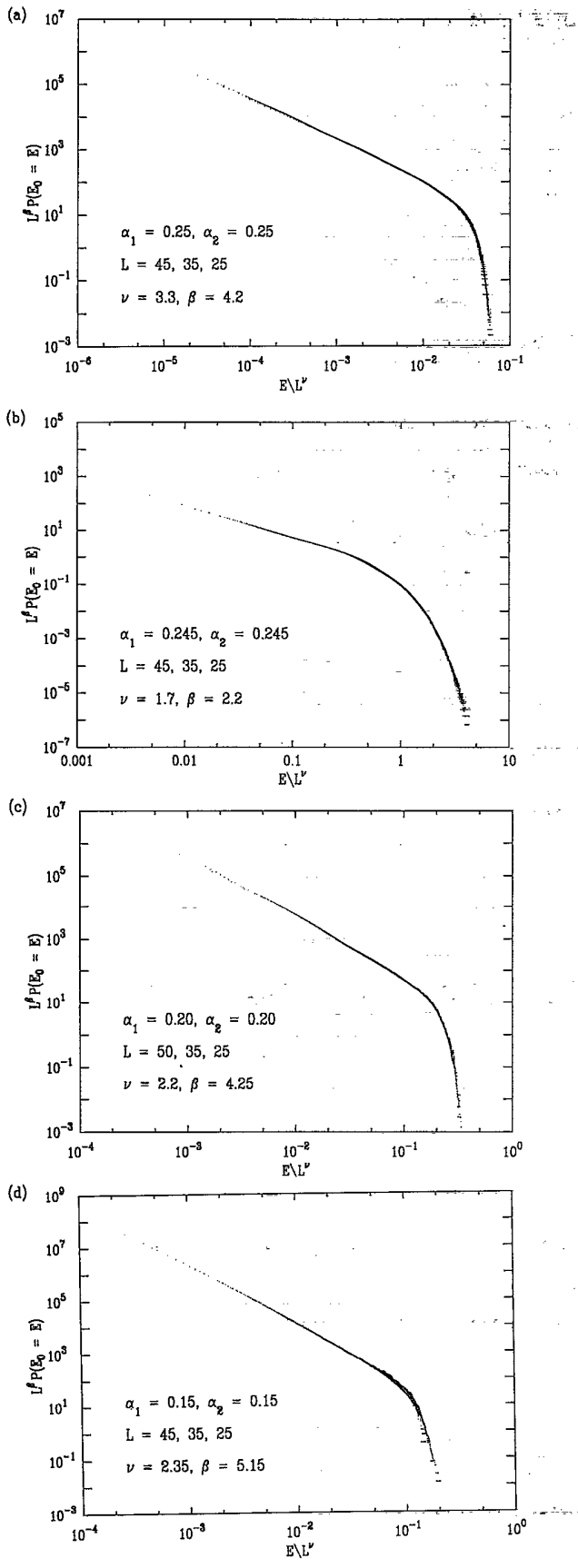

FIG. 4. Finite-size scaling for various α values. We present results for $\alpha=0.25$, 0.245, 0.20, and 0.15 in (a)–(d), respectively. The scaling results are summarized in Table I.

paper are based on statistics derived from 10 000 000–50 000 000 avalanches.

A. The isotropic model with open boundary condition

We discuss in this section the behavior of the system with open boundary conditions along the line $\alpha_1=\alpha_2=\alpha$ (see Fig. 2). The model displays SOC for $\alpha\geq 0.05$. However, the critical exponents change as a function of α. We present the dependence of the exponent B on α in Fig. 3. We did a detailed finite-size scaling for the values $\alpha\geq 0.10$. Below this α value, the exponent B is too large to obtain proper statistics of the cutoff behavior. We present in Fig. 4 four examples of finite-size scaling for the α values 0.25, 0.245, 0.20, and 0.15, respectively. As seen in those graphs, finite-size scaling works very well. This verifies the criticality of the system. No correlation length is introduced by the nonconservation. We show in Fig. 5 results for the dependence of the critical exponents ν and β on α in the region $0.10\leq\alpha\leq 0.25$.

Since the avalanches are completely localized for $\alpha=0$, we know that a localization transition should occur at some $\alpha\geq 0$. Indeed, we see such a transition at approximately $\alpha=0.05$. Below this level, the distribution function becomes localized. A system-size-independent exponential length scale appears in the distribution of avalanche sizes. The transition seems discontinuous, i.e., the length scale does not change continuously near the transition.

The exponent B changes continuously in the range $0.05\leq\alpha\leq 0.25$. However, for the scaling indices we see a very sharp transition between the conservative and nonconservative regimes. The scaling index ν drops from 3.3 to 1.8 when changing α from 0.25 to 0.245. We attribute this change of scaling to a transition in the temporal behavior of the avalanches. Introduce the integrated amount of local activity in the avalanche as a third dimension. When the system is conservative, the avalanches have the shape of a cone, where the height is approximately of the same scale as the radius. However,

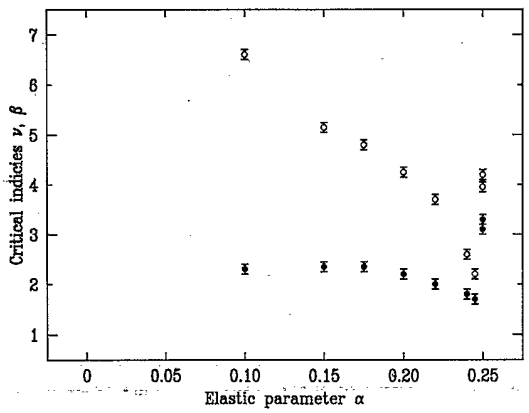

FIG. 5. The critical indices ν (solid symbols) and β (open symbols) as functions of the conservation. Notice the sharp transition when a small nonconservation is introduced. The error bars represent a mistake of 0.10 in the exponents.

TABLE I. The critical exponents for the isotropic system with open boundary conditions. The scaling relation, Eq. (6), is fulfilled within numerical accuracy (except for $\alpha=0.22$). For comparison we also list the critical exponents for the original BTW model.

Model	$1+B$	ν (± 0.10)	β (± 0.10)	β/ν
$\alpha=0.25$	1.22 ± 0.05	3.3	4.2	1.27 ± 0.05
$\alpha=0.2499$	1.22 ± 0.05	3.1	3.95	1.27 ± 0.06
$\alpha=0.245$	1.17 ± 0.05	1.7	2.2	1.29 ± 0.11
$\alpha=0.24$	1.25 ± 0.05	1.8	2.6	1.44 ± 0.11
$\alpha=0.22$	1.65 ± 0.05	2.0	3.7	1.85 ± 0.13
$\alpha=0.20$	1.89 ± 0.10	2.2	4.25	1.93 ± 0.12
$\alpha=0.175$	2.06 ± 0.10	2.35	4.8	2.04 ± 0.12
$\alpha=0.15$	2.22 ± 0.10	2.35	5.15	2.19 ± 0.13
$\alpha=0.10$	2.72 ± 0.10	2.3	6.6	2.87 ± 0.18
BTW, locally	1.1 ± 0.05	2.0	2.3	1.15 ± 0.08
BTW, globally	1.1 ± 0.05	2.0	2.3	1.15 ± 0.08

when the system is nonconservative, even the smallest dissipation level would define a maximal number of relaxation at a given site. Therefore, the avalanches will become flat. This implies a change in the scaling behavior of the avalanches from 3 to 2. We believe that the width of the transition will depend on the system size. Another interesting feature in the nonconservative region of the model is that although the exponent B changes strongly, ν is almost a constant. Still, the relationship between the exponents, Eq. (6), is fulfilled in all the measured region.

It is worth noting that at each relaxation in the Feder model (with dynamical noise and $F_{\rm th}=4$), the effective α is $1/F_{i,j}$. Thus we can estimate the level of conservation by measuring the average over a large number of relaxations. We find $\alpha\simeq0.217$, and indeed, the exponent and the scaling indices are consistent with the point $\alpha\simeq0.217$ in our model (with open boundary conditions). Another interesting comparison is with the BTW model with global and local driving. We present all the results in Table I. While the difference in B is very small, there is a dramatic change in the scaling exponents ν and β.

B. Different boundary conditions

The data that we presented in Sec. III A imply that there is a dependence of the exponents on the parameters of the model. It is also well known that existence of criticality depends on the boundary conditions. A model with BTW dynamics and reflecting boundary conditions (conservative), for example, cannot display any critical behavior. However, no systematic study of this issue was done even for the original BTW model. In this section we show that the results depend very strongly on the boundary conditions.

First, we choose the physically interesting case of the free boundary conditions. In Fig. 6 we show the change of the exponent B as the level of conservation is changed for the model with free boundary conditions (note that the free boundary conditions are totally reflective for the conservative case so the model obviously cannot display criticality). In Fig. 7 we display the dependence for both the free and the open boundary conditions. The change in the boundary conditions induces a dramatic change in

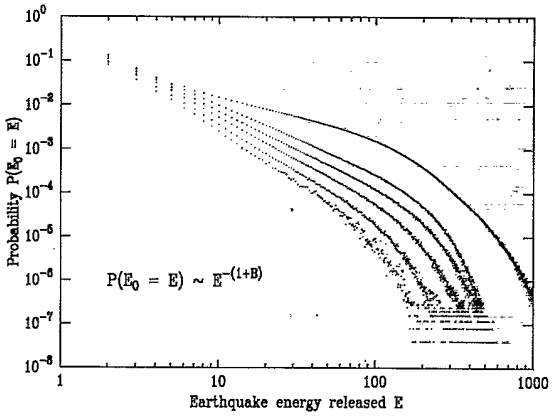

FIG. 6. Simulation results for a 35×35 system with free boundary conditions. Different curves refer to different levels of conservation. The slopes of the curves become steeper as the α values are decreased. The graphs correspond to $\alpha=0.245$, 0.20, 0.15, 0.10, 0.05, and 0.01, respectively.

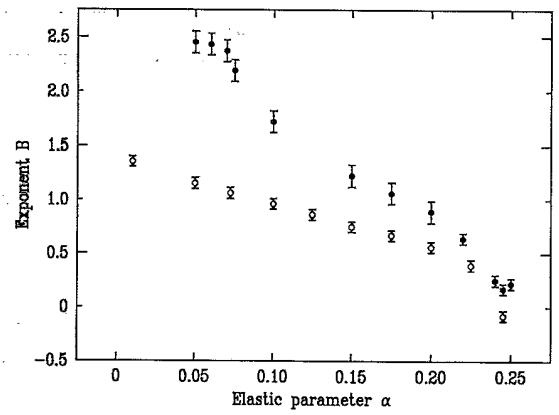

FIG. 7. The power-law exponent B as a function of the elastic parameter α defined in Eq. (3). Solid symbols correspond to the model with open boundary conditions. The measured B values for the model with free boundary conditions are displayed as open symbols.

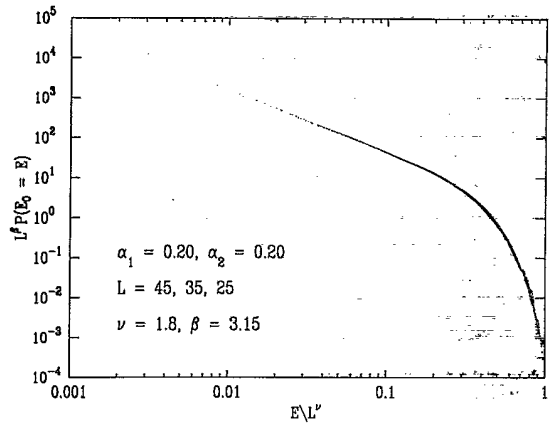

FIG. 8. Finite-size scaling for the model with free boundary conditions and $\alpha=0.20$.

the exponents. The exponents for the free boundary conditions are much lower than for the open boundary conditions. Also, the localization transition for the free boundary conditions is lowered to $\alpha\simeq 0.01$.

We did a finite-size-scaling analysis for one point along this line, for $\alpha=0.20$. Finite-size scaling seems to work very well in this case also, as is shown in Fig. 8.

To check this dependence more carefully, we changed the boundary conditions at the edge continuously from open boundary conditions $\alpha_{\rm BC}=\alpha$ to reflecting boundary conditions $\alpha_{\rm BC}=\frac{1}{3}$. We see a continuous change of the exponent B when going from the open boundary conditions, $\alpha_{\rm BC}=0.20$ to a value of $\alpha_{\rm BC}\simeq 0.28$, which is larger than the $\alpha_{\rm BC}=\alpha/(1-\alpha)=0.25$ used for free boundary conditions. Above this value, the systems seems to be noncritical in the sense that no power laws are seen. The distribution function can no longer be scaled with system size, although the size of the maximal avalanches scale with system size. We have observed similar behavior for other bulk values of α, but we did not make a detailed study.

IV. RELATION TO EARTHQUAKES

In nature, earthquakes are probably the most relevant paradigm of self-organized criticality. In 1956 Gutenberg and Richter realized that the rate of occurrence of earthquakes of magnitude M greater than m is given by the relation

$$\log_{10}N(M>m)=a-bm\ , \tag{7}$$

where a and b are constants for a given fault. This is the Gutenberg-Richter law [14]. Measurements of the parameter b yield a wide range of values for different faults. Values of b from 0.80 to 1.06 for small earthquakes and 1.23 to 1.54 for large earthquakes have been recorded [15].

The energy (seismic moment) E released during the earthquake is believed to increase exponentially with the earthquake magnitude,

$$\log_{10}E=c+dm\ , \tag{8}$$

where the parameter d is 1 and $\frac{3}{2}$ for small and large earthquakes, respectively [16]. Thus the Gutenberg-Richter law is transformed into a power law for the number of observed earthquakes with energy greater than E:

$$N(E_0>E)\simeq E^{-b/d}=E^{-B}\ , \tag{9}$$

Note that B is in the *same* range for both small and large earthquakes, namely, 0.80–1.05, but it is not a universal exponent. In our model we measured the distribution function, Eq. (4). This explains why we use the notation $(1+B)$ for the power-law exponent.

The idea of explaining the Gutenberg-Richter law by such a two-dimensional model was already proposed by Otsuka [17]. It was also suggested independently by several authors [12,13,18–20] immediately after the introduction of the idea of SOC by Bak *et al.* that SOC might be a good explanation for the observed power laws. Most of those suggested models are conservative and have no physical interpretation in the context of the driven spring-block model. Furthermore, since the models are conservative, they predict unique power-law exponents which are much lower then the observed values ($B\simeq 0.10$).

If the different elastic constants K_1, K_2, and K_L are within the same scale, the characteristic value of α for earthquakes is 0.20, which amounts to a B value around 0.9 in the case of open boundary conditions. The reported values of B are indeed in this range. Thus our results, apart from providing an explanation for the observed power laws, also give some explanation for the observed variability. One should not look for universal values of B in nature.

Another interesting connection of this model to earthquakes is that, like real earthquakes, it displays spatiotemporal correlations between the earthquakes. Those aspects are discussed in some detail elsewhere [10]. This gives us good reason to believe that this simplistic picture has a real connection to the actual fault dynamics that leads to earthquakes.

V. THE ANISOTROPIC CASE

As mentioned earlier, we can control the anisotropy in the system while keeping the level of conservation constant. We changed the ratio α_1/α_2 from 1 to 0 while keeping $2\alpha_1+2\alpha_2=C$, where C is a constant (see Fig. 2). We measured the distribution function for fixed conservation levels from $C=0.90$ to 0.50. The change in B is negligible. The system is critical, except for the case of the one-dimensional system where the distribution function is no longer a power law. In Fig. 9 we show a representative example of distribution functions that are derived for $C=0.80$. For this particular value of C we also measured the scaling exponents. We present the data in Table II. The finite-size-scaling exponent ν changes continuously from 2.2 to 1. This is the signature of the rising anisotropy in the model. The surprising minimal change in the exponent B is due to constant con-

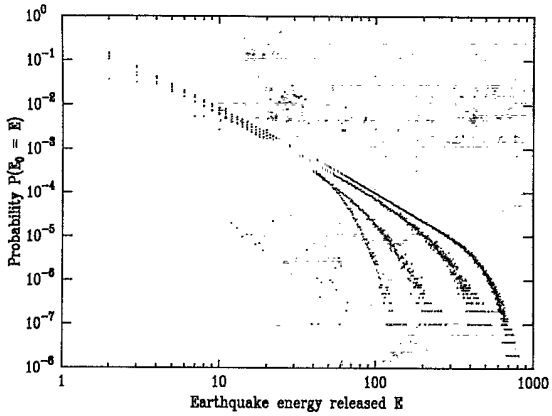

FIG. 9. Size distribution functions for the anisotropic case scanned along a constant conservation level, $C=0.80$ (see Fig. 2). The anisotropic ratios are 1, $\frac{3}{5}$, $\frac{1}{3}$, $\frac{1}{7}$, and 0. They are easily recognized by the decrease of the cutoff in the maximal avalanche size. Notice that the one-dimensional distribution has no resemblance to the rest, even though the largest avalanches scale as L.

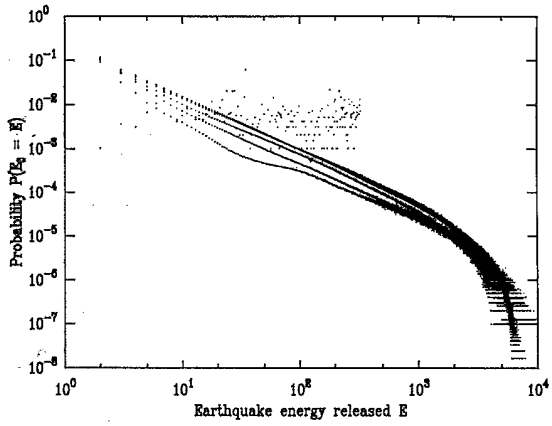

FIG. 10. Size distribution functions for the anisotropic case in a conservative model, $C=1$. The anisotropic ratios are 1, $\frac{2}{3}$, $\frac{3}{7}$, $\frac{1}{4}$, $\frac{1}{9}$, and 0. Notice that the cutoffs are not modified as in the nonconservative model. The scaling is modified to 2 in the one-dimensional case.

servation. Even for large anisotropy, there is still a strong interaction between the lines in the system. The reason is the large activity of the one-dimensional avalanches, so the avalanches remain two dimensional. However, the avalanches become stretched in the preferred direction, which is the reason for the change of ν.

Thus, the general result for the two-dimensional nonconservative case is that the anisotropy has almost no effect on the power-law exponent. However, the scaling exponent ν changes continuously from a two-dimensional to a one-dimensional scaling of the avalanches.

In the conservative case $C=1$, we observe some different effects. The results for the conservative case are presented in Fig. 10. At very large anisotropy the curve separates into two parts. The lower part with a higher slope seems to be related to one-dimensional avalanches, while the long-range behavior is still with the same power law as the isotropic case. Again, this is a result of the extremely high activity of one-dimensional avalanches. A discontinuous transition to the one-dimensional case appears. As in the isotropic case, the transition from the conservative to the nonconservative part results in a discontinuous transition in the values of the ν.

TABLE II. The critical indices for the anisotropic system with open boundary conditions. Note that even though Fig. 9 shows an almost negligible change in the power-law exponent, the ratio β/ν varies a lot and does not fulfill the scaling relation, Eq. (6).

Model	ν (± 0.10)	β (± 0.10)	β/ν
$(\alpha_1,\alpha_2)=(0.20,0.20)$	2.2	4.25	1.93 ± 0.12
$(\alpha_1,\alpha_2)=(0.15,0.25)$	2.0	4.4	2.37 ± 0.13
$(\alpha_1,\alpha_2)=(0.10,0.30)$	1.6	3.8	2.37 ± 0.21
$(\alpha_1,\alpha_2)=(0.05,0.35)$	1.1	2.8	2.55 ± 0.33

VI. CONCLUSIONS

The main results in this paper are the following.

(1) Nonconservative models can organize themselves to a critical state. Apart from a relatively small localized region, the nonconservative model displays SOC for all conservation levels. This is seen only for models that are driven globally. Local drive together with nonconservation introduces a system-size-independent length scale (i.e., if the local drive is so large that it destroys the correlation in the lattice).

(2) The self-organization is very sensitive to the boundary conditions. The critical exponents and scaling indices change as the boundary conditions are modified. However, this model displays SOC for a wide range of possible boundary conditions.

(3) While SOC is a very stable feature of this model, the exponents are not universal. The exponent B changes continuously when changing the level of conservation. Also, the boundary has an effect on the power-law exponent B. However, the anisotropy does not influence the value of B as long as the level of conservation is constant. The scaling exponents are changed in all the above cases.

(4) We observe several phase transitions in the system. We see a transition when going from a conservative to a nonconservative system. It manifests itself by a discontinuous change in the critical indices ν and β. The observed width of the transition is a finite-size effect. Another transition takes place at low α when the avalanches become localized. Finally, a transition from a critical to a noncritical system is seen when the anisotropy grows very large (the system become effectively one dimensional).

Clearly, the existence of criticality in nonconservative models implies that strong correlations are induced in the system by a self-organization process. Otherwise, avalanches would become completely localized for any nonconservation. To illustrate the self-organization procedure, we present the running average of earthquake

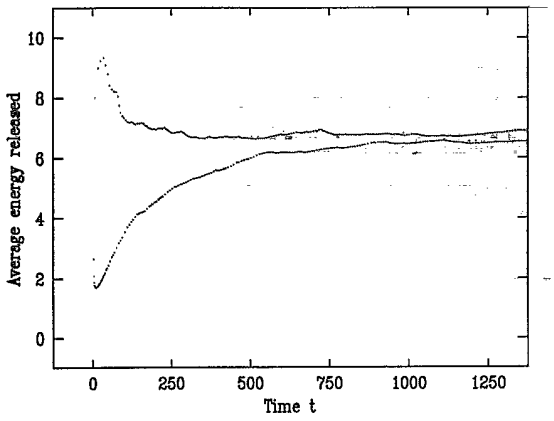

FIG. 11. The average size of the avalanches as a function of time during the self-organization process. System size $L=70$, conservation level $\alpha=0.20$, and open boundary conditions. The lower graph presents the rise of the average for an initial random lattice. It is a measure of the rise of the correlation length in the system. The saturation is a result of the finite system size. The upper graph presents data for an initially correlated lattice. The fluctuations in the beginning of both graphs are a result of the low exponent of this distribution function (the larger avalanches define the average).

sizes in Fig. 11. We start from a random uncorrelated configuration. The average grows gradually, indicating the autocorrelation of the system into the critical state. Since the system autocorrelates slowly, the maximal sizes of avalanches grow slowly. This growth is limited only by the system size, which defines the avalanche-size cutoff. On the other hand, if we start with a correlated system, the average will immediately stabilize into the system-size-dependent value. This is also shown in Fig. 11.

The avalanches are generated by correlated clusters of sites, which in turn are generated by the avalanches. The correlated clusters are modified by interactions with other clusters through avalanches. Another organization process is that the boundary acts as a source of correlation. The evidence for this is the effect of boundary conditions on the critical exponents.

A change in the parameters of the models will not destroy the self-organization process, but will modify it strongly. That is the origin for our results. A more detailed picture of this organization can be easily derived in one dimension, where the boundary between clusters is a point and not a line.

With this in mind, it is easy to understand why no criticality is seen for models, which are driven locally. The local perturbations will destroy the correlations in the system. This interpretation can be tested numerically in our model. The system should be resistant to noise, which will not destroy the correlations. On the other hand, the model should display localization if the noise is so large that it can destroy the correlations. And indeed it does behave in this way.

We have proved the nonuniversality of the self-organization process for our model. However, as we noted before, exponents will be modified even for the original BTW model when the boundary condition is changed or when introducing symmetry-preserving modifications in the algorithm. So our basic conclusions seem to also be relevant to other self-organizing systems. We believe that the main theoretical effort in this field should be dedicated to the understanding of the common features of the self-organization, rather than to looking for universality in the results.

ACKNOWLEDGMENTS

We would like to thank Per Bak for valuable discussions of this subject. Also, we would like to express our gratitude to Jens Feder for allowing us to use one of his computers rather intensively. K.C. gratefully acknowledges the financial support of Carlsbergfondet and Emil Herborgs Legat. Z.O. thanks the Weizmann and Fullbright Foundations for support during this research. Both authors appreciate the support and hospitality of Brookhaven National Laboratory. This work was supported by the Division of Basic Energy Sciences, U.S. DOE, under Contract No. DE-AC02-76CH00016.

APPENDIX A

Assume the force on a block at position (i,j) is above the threshold value, that is

$$F_{\rm th} \le F_{i,j} = K_1[2x_{i,j} - x_{i-1,j} - x_{i+1,j}] + K_2[2x_{i,j} - x_{i,j-1} - x_{i,j+1}] + K_L x_{i,j} \ . \tag{A1}$$

If $\bar{x}_{i,j}$ denotes the displacement of block (i,j) from the relaxed position after the block has slipped to zero-force position, then

$$0 = K_1[2\bar{x}_{i,j} - x_{i-1,j} - x_{i+1,j}] + K_2[2\bar{x}_{i,j} - x_{i,j-1} - x_{i,j+1}] + K_L \bar{x}_{i,j} \ , \tag{A2}$$

where we exploit the fact that nearest-neighbor blocks of (i,j) cannot be supercritical at the same time, i.e.,

$$x_{i\pm1,j} = \bar{x}_{i\pm1,j} \ , \qquad x_{i,j\pm1} = \bar{x}_{i,j\pm1} \ . \tag{A3}$$

The slipping block (i,j) affects the force on nearest-neighboring blocks. As an example, we calculate the change of force on block $(i,j+1)$. The force on block $(i,j+1)$ is

$$F_{i,j+1} = K_1[2x_{i,j+1} - x_{i-1,j+1} - x_{i+1,j+1}] + K_2[2x_{i,j+1} - x_{i,j} - x_{i,j+2}] + K_L x_{i,j+1} \ . \tag{A4}$$

Thus the change of force due to a slip at position (i,j) is

$$\delta F_{i,j+1} = -K_2 dx_{i,j} \ . \tag{A5}$$

Notice that the force on block $(i,j+1)$ may very well be affected by a slip at position $(i,j+2)$ but that does not interfere with this argument. An expression for the change

in displacement of block (i,j),

$$dx_{i,j}=\tilde{x}_{i,j}-x_{i,j} \ , \tag{A6}$$

is obtained by subtracting Eq. (A1) from Eq. (A2),

$$0-F_{i,j}=[2K_1+2K_2+K_L]dx_{i,j} \ . \tag{A7}$$

Finally, substituting Eq. (A7) into Eq. (A5), we find

$$\delta F_{i,j+1}=\frac{K_2}{2K_1+2K_2+K_L}F_{i,j} \ . \tag{A8}$$

APPENDIX B

The boundary condition is *free* if the blocks in the boundary layer are connected only to blocks within the fault, i.e., the force on a boundary block, say, at site (i,L), is given by

$$F_{i,L}=K_1[2x_{i,j}-x_{i-1,j}-x_{i+1,j}] +K_2[x_{i,j}-x_{i,j}-1]+K_L x_{i,j} \ . \tag{B1}$$

If this blocks slips, we find

$$0-F_{i,L}=[2K_1+K_2+K_L]dx_{i,L} \ , \tag{B2}$$

resulting in

$$\delta F_{i\pm1,L}=\frac{K_1}{2K_1+K_2+K_L}F_{i,L}=\alpha_{\rm BC}F_{i,L} \ . \tag{B3}$$

If the model is isotropic, $K_1=K_2=K$, then

$$\alpha=\frac{K}{4K+K_L} \ . \tag{B4}$$

We can express the elastic ratio $\alpha_{\rm BC}$ used when boundary blocks slip in terms of the bulk α,

$$\alpha_{\rm BC}=\frac{\alpha}{1-\alpha} \ . \tag{B5}$$

If a block in one of the corners slips, we use

$$\alpha_{\rm BC}=\frac{\alpha}{1-2\alpha} \ . \tag{B6}$$

For a simulation of the model with *open* boundary conditions, we use the same α all over the lattice. That is, if block (i,L) slips, we increase the force on the three neighboring blocks $(i\neq1,L)$ with an amount equal to $\alpha_{\rm BC}F_{i,L}$, where $\alpha_{\rm BC}=\alpha$ is defined in Eq. (3).

*Permanent address: Institute of Physics and Astronomy, University of Aarhus, DK-8000 Aarhus C, Denmark.

[1] P. Bak, C. Tang, and K. Wiesenfeld, Phys. Rev. Lett. **59**, 381 (1987).
[2] T. Hwa and M. Kardar, Phys. Rev. Lett. **62**, 1813 (1989).
[3] G. Grinstein, D.-H. Lee, and S. Sachdev, Phys. Rev. Lett. **64**, 1927 (1990).
[4] S. S. Manna, L. B. Kiss, and J. Kertész, J. Stat. Phys. **61**, 923 (1990).
[5] H. J. S. Feder and J. Feder, Phys. Rev. Lett. **66**, 2669 (1991).
[6] L. P. Kadanoff, L. Nagel, L. Wu, and S. Zhou, Phys. Rev. A **39**, 6524 (1989).
[7] S. S. Manna, J. Phys. A **24**, L363 (1991).
[8] Z. Olami and K. Christensen (unpublished).
[9] Z. Olami, H. J. S. Feder, and K. Christensen, Phys. Rev. Lett. **68**, 1244 (1992).
[10] K. Christensen and Z. Olami, J. Geophys. Res. (to be published).
[11] R. Burridge and L. Knopoff, Bull. Seismol. Soc. Am. **57**, 341 (1967).
[12] P. Bak and C. Tang, J. Geophys. Res. **94**, 15 635 (1989).
[13] P. Bak and K. Chen, in *Fractals and Their Uses in Earth Sciences*, edited by C. C. Barton and P. R. Lapointe (Geological Society of America, Boulder, CO (1990).
[14] B. Gutenberg and C. F. Richter, Ann. Geofis. **9**, 1 (1956).
[15] J. F. Pacheco, C. H. Scholz, and L. R. Sykes, Nature **355**, 71 (1992).
[16] G. Ekström and A. M. Dziewonski, Nature **332**, 319 (1988).
[17] M. Otsuka, Phys. Earth Planet. Inter. **6**, 311 (1972).
[18] J. M. Carlson and J. S. Langer, Phys. Rev. Lett. **62**, 2632 (1989).
[19] K. Ito and M. Matsuzaki, J. Geophys. Res. **95**, 6853 (1990).
[20] S. R. Brown, C. H. Scholz, and J. B. Rundle, Geophys. Res. Lett. **18**, 215 (1991).